SAND2014-4936J

Application of Electrically Invisible Antennas to the Modulated Scatterer Technique

Dylan A. Crocker, *Student Member, IEEE*, and Kristen M. Donnell, *Senior Member, IEEE*

***Abstract*—The Modulated Scatterer Technique (MST) has shown promise for applications in microwave imaging, electric field mapping, and materials characterization. Traditionally, MST scatterers are dipoles centrally loaded with an element capable of modulation (e.g., a PIN diode). By modulating the load element, signals scattered from the MST scatterer are also modulated. However, due to the small size of such scatterers, it can be difficult to reliably detect the modulated signal. Increasing the modulation depth (a parameter related to how well the scatterer modulates the scattered signal) may improve the detectability of the scattered signal. In an effort to improve the modulation depth, the concept of electrically invisible antennas is applied to the design of MST scatterers. This paper presents simulations and measurements of MST scatterers that have been designed to be electrically invisible during the reverse bias state of the modulated element (a PIN diode in this case), while producing detectable scattering during the forward bias state (i.e., operate in an electrically visible state). Results using the new design show significant improvement to the modulation depth of the scattered signal as compared to a traditional MST scatterer (i.e., dipole centrally loaded with a PIN diode).**

***Index Terms*—dual-loaded scatterer, invisible antennas, microwave imaging, modulated scatterer technique, modulation depth**

I. Introduction

THE Modulated Scatterer Technique (MST) has shown potential for microwave imaging, electric field mapping, and materials characterization applications [1]-[4]. The technique is based on irradiating a small scatterer (typically a resonant dipole centrally loaded with a PIN diode) with an electromagnetic wave. This incident wave induces a current on the dipole, corresponding to its geometry and local environment, which subsequently causes scattering [5]. Loading the dipole antenna with a PIN diode enables the dipole impedance to be (electronically) changed by modulating the PIN diode bias between the forward and reverse states in a controlled manner. In this way, the scattering from the dipole will also be modulated and can be uniquely distinguished from the scattering of other objects [1]. More specifically, signal detection is improved with modulation since modulated signals are distinct from non-coherent clutter present in the environment and noise in the detection system. Additionally, with regard to an array of MST scatterers, modulation allows an array element to "tag" its own signal, providing a means for spatial identification of the location from which the signal is received.

Recently, a new MST scatterer design was proposed (primarily for embedded sensing applications including materials characterization), consisting of a dual-loaded dipole scatterer, referred to as a dual-loaded scatterer, or DLS [6]-[7]. A schematic of the traditional MST scatterer and DLS is provided in Fig. 1. The DLS differs from the conventional MST scatterer as it is loaded with two PIN diodes instead of one, each offset from the center by a distance d_z.

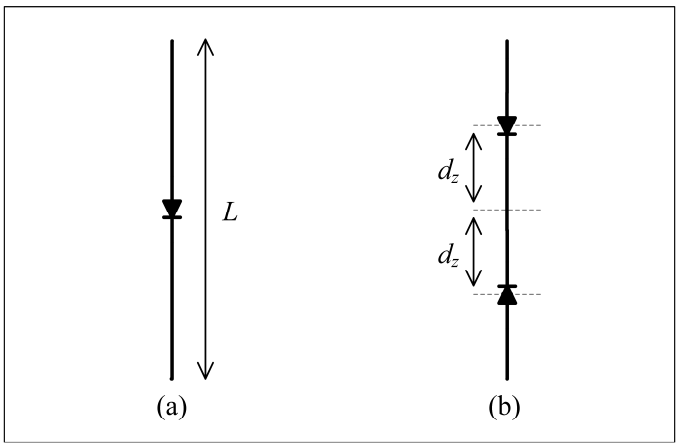

Fig. 1. Schematic of MST elements: (a) Traditional MST scatterer, (b) recently proposed dual-loaded MST scatterer (DLS).

The dual-loading results in four possible (modulation) states of the scatterer (as opposed to two for traditional MST scatterers). For materials characterization, the scattered signal from all four states can be used, together in the form of a differential ratio calculation, to remove unwanted signals (common to all states, including the carrier signal) from the total detected signal [8].

In either configuration (single or dual loaded), the MST scatterer is usually quite small and therefore the (modulated) scattering is also quite small. Increasing the capability of the scatterer to modulate the scattered signal would make this technique more robust. One method used to describe the modulation capability of a scatterer is through a quantity known as modulation depth (MD).

The work of D. A. Crocker was supported by Sandia National Laboratories through their Critical Skills Master's Program.

D. A. Crocker is with Sandia National Laboratories, Albuquerque, NM 87185 (e-mail: dylan.crocker@sandia.gov).

K. M. Donnell is with the Applied Microwave Nondestructive Testing Laboratory (*amntl*), Electrical and Computer Engineering Department, Missouri University of Science and Technology, Rolla, MO 65409 USA (e-mail: kmdgfd@mst.edu).

Modulation depth is a dimensionless quantity defined as the amplitude ratio of the power in the modulated signal to the power in the carrier, expressed as a percentage [9]. It can also be defined as a signal amplitude ratio (e.g., S-parameters or electric field) [9]. For the purposes of this work, MD will be determined in terms of signal amplitude and calculated as shown below in (1):

$$MD = \frac{A-B}{A+B} * 100\% \quad (1)$$

where A is the maximum peak-to-peak amplitude of the scattered electric field, and B is the minimum peak-to-peak amplitude of the scattered electric field [9]. MD is useful to consider with respect to modulated scatterers since it quantifies how well a scatterer can modulate the scattered signal. Practically (as mentioned above), the signal scattered by an MST scatterer is typically very small (e.g., scattering from a resonant dipole). As a result, the residual carrier (i.e., the incident signal present in the scattered signal) can significantly limit the dynamic range of a detection system [10]. Furthermore, the mutual coupling between elements of different modulation states within an array of MST scatterers can result in far-field calculation errors [10]. Improving the MD may help mitigate these detection issues, since an increase in the MD indicates an increase in the relative power of the modulated signal to that of the carrier, thus decreasing the required sensitivity of the detection system. Consequently, weak scattering objects (such as MST scatterers) may be more reliably detected [11]. Such an approach has been applied in the Radio Frequency Identification (RFID) regime to improve and optimize the performance (operating range, data rate, etc.) of RFID tags [12]-[13].

The concept of improving MD has also been applied for increasing the robustness of MST. In [14], in order to maximize the MD, a printed dipole with length, *L,* of λ/10 (see Fig. 1) was centrally loaded with an optical diode which was conjugate matched (during the forward biased state) to the input impedance of the dipole. Another technique was proposed in [11] in which changes to physical parameters of an MST element (scatterer length, etc.) and the addition of matching networks to the load impedance were considered to optimize scattering and subsequently improve MD. In this investigation, the concept of electrically invisible antennas [15]-[19] is applied to the design of MST scatterers in order to improve the MD. Previous work has shown that electrically invisible antennas have application in reduction of radar cross section [20], frequency-selective surfaces [21], reconfigurable antennas [16], [19], as well as reduction in mutual coupling between array elements [15]. Considering these applications with respect to MST, it is proposed that by designing an MST scatterer that can operate in electrically visible (i.e., scattering) and invisible (i.e. minimum/zero scattering) states, the MD may be enhanced. This concept was first proposed in [22] and is further investigated and extended herein.

Building on the DLS design (illustrated in Fig. 1) mentioned above, this paper focuses on the integration of electrically invisible antennas and the DLS. By choosing the loading characteristics of the DLS (i.e., load location and type) in a specific way, the DLS can be designed to be electrically invisible, herein known as the IDLS. For this work, an IDLS is designed to have one fixed load (e.g., a lumped element), and one load capable of modulation (e.g., a PIN diode). In this way, the IDLS will have two states (similar to the conventional single-loaded MST element), but one state will cause the IDLS to be electrically invisible. In other words, the IDLS will have the capability to be modulated between an electrically visible and invisible state, thereby improving the MD. As such, incorporating the IDLS into MST may improve the overall robustness and practicality of this technique.

For the purposes of this analysis, electromagnetic simulations, based on the Method-of-Moments (MM), were developed to calculate the current induced on linear MST scatterers (loaded dipoles) from a normally incident plane wave [23]-[25]. The MM simulations solve Pocklington's Electric Field Integral Equation (EFIE) which has been simplified using thin-wire approximations [23]. For improved accuracy of practical wire diameters, an extended thin-wire approximation to the Pocklington EFIE kernel was utilized [26].

Simulations and measurements of a new MST scatterer that has been designed to be electrically invisible during one modulation state are provided in subsequent sections of this paper. Additionally, the performance (i.e., MD) of the new design is compared to a traditional MST scatterer (a half-wave dipole centrally loaded with a PIN diode) to illustrate the improvement offered by this new approach.

II. Invisible Single Loaded Scatterer

In order to fully understand the application of electrically invisible antennas to MST, initially a centrally-loaded dipole, herein referred to as a single-loaded scatterer (SLS), was studied. According to [15], zero scattering (i.e. electrical invisibility) is achieved by loading a dipole scatterer with an inductive reactance which causes a 180° phase shift in the current induced on the scatterer in the vicinity of the load. When this reactance is chosen properly, the resulting phase shift causes the integral of the current induced along the SLS to approach zero [15], thereby minimizing the scattering of the SLS and achieving electrical invisibility [17].

Using the developed simulations, various inductive loads were considered in order to determine the optimal load for electrical invisibility of an SLS of length, *L*, 60 mm (λ/2 at 2.5 GHz) and diameter 0.511 mm (24 AWG). The particular wire size of 24 AWG was chosen because it provides a good balance between (practical) usability and dimensions for the thin-wire approximation employed by the simulations. A design frequency of 2.5 GHz was chosen for correlation to measurements discussed below in section IV. The simulated excitation of the scatterer was a normally-incident plane wave of unity magnitude, polarized along the length of the scatterer. All subsequent simulations also use this basic geometry (wire length and diameter) and excitation. Fig. 2 shows the resulting broadside (monostatic) scattering, E_s, at a distance of 1.5 m

from the scatterer as a function of load impedance. All scattering simulations presented herein were calculated monostatically at a broadside distance of 1.5 m (far-field region) from the scatterer.

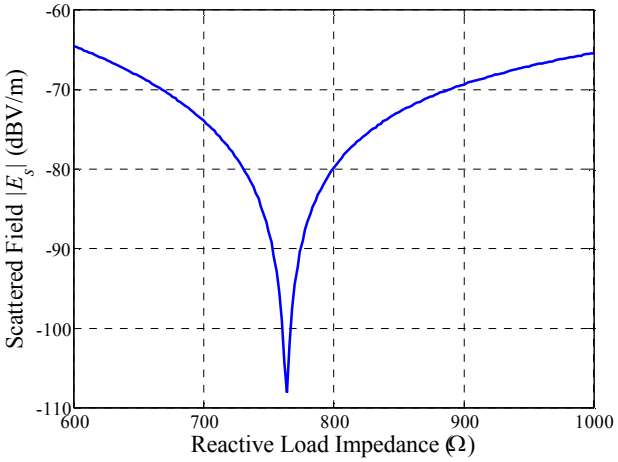

Fig. 2. Scattering from an SLS centrally loaded with an ideal inductor as a function of load reactance.

As shown in Fig. 2, when a reactive (inductive) load of ~764 Ω (corresponding to an inductance of 48.6 nH at the design frequency) is placed at the center of the dipole, the magnitude of the scattered field, $|E_s|$, is significantly reduced, indicating that the scattered field approaches zero (i.e., the SLS is electrically invisible). It should be noted here that $|E_s|$ is also significantly reduced by other reactance values; however, the optimal load is defined at the point of minimal scattering, herein referred to as the scattering null. To illustrate the effect of the inductive load, the current induced along the length of the scatterer for this design is shown in Fig. 3. The current induced on an open-circuited (i.e., high impedance load) SLS, of the same geometry, is also included for comparison.

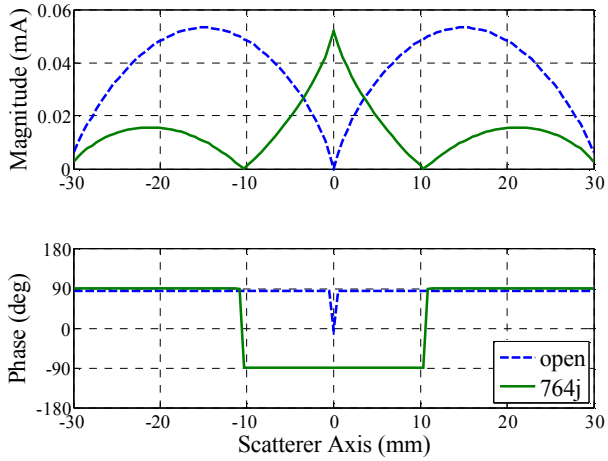

Fig. 3. Distribution of current induced on an open-circuited and reactively loaded SLS.

As can be seen from Fig. 3, the (approximate) 180° phase shift [15] (mentioned above) is evident through the central region of the reactively loaded SLS current distribution (solid line). As previously discussed, the phase shift results in the integral of the current distribution approaching zero (similar to the integral of a sine wave period) which results in a scattering null. In contrast, the current induced along the length of the open-circuited SLS (dashed line) has relatively uniform phase, hence the integral of the induced current (and the subsequent scattering) does not approach zero.

It is interesting to note that the invisible SLS (or ISLS) may have practical applications related to materials characterization. Considering the results in Fig. 2, if any physical or operating parameters were to change (frequency, load impedance or location, dipole length, properties of the material surrounding the ISLS, etc.), the condition for electrical invisibility would also change. To this end, such a scatterer may be designed to purposely lose (or gain) invisibility as a result of environmental (e.g. material property) changes. For example, a similar ISLS was designed to be invisible at 2.5 GHz in mortar (relative complex dielectric properties, ε_r, assumed to be 4 - j0.1). To achieve electrical invisibility for this case, an inductive load of 33.24 nH was required.

Simulations were conducted to vary the relative permittivity (i.e., the real part of ε_r) that may result from changes in the material; for example, cracks may occur which may cause the permittivity to reduce, or the ingress of chloride or moisture may cause the permittivity to increase. The results of this simulation are shown in Fig. 4.

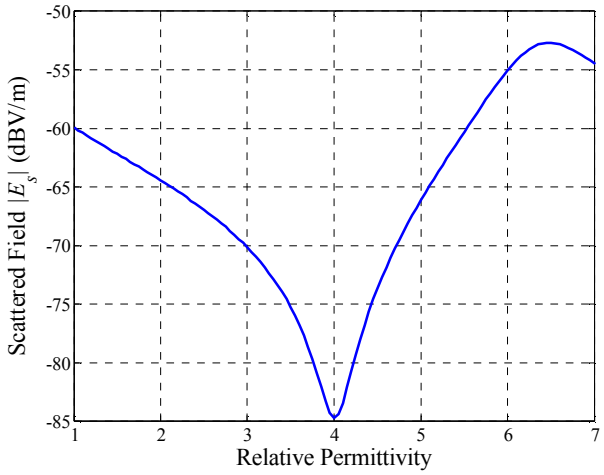

Fig. 4. Scattering from an ISLS designed for invisibility in mortar as a function of relative permittivity.

As expected and evident in Fig. 4, the scattered field of the ISLS is sensitive to changes in the surrounding material. Therefore, a scatterer may be designed to become visible if the permittivity in the vicinity of the probe decreases (for example, due to cracking), or increases (possibly due to the presence of moisture). Unfortunately, the ISLS cannot be modulated, making detection more challenging if the expected (visible response) is not *a priori* known. This indicates

improvements to the design may offer practical benefits. An additional, practical concern is the magnitude of the scattered field itself. In order to reliably detect changes in E_s on the order of that shown in Fig. 4, sensitive (expensive/complex) detection equipment may be required.

To this end, the addition of modulation capability to the ISLS may render an improved and move robust scatterer design useful for other MST applications [1] as well. As such, the IDLS design (mentioned above), which maintains the ability to modulate between visible and invisible states, is considered next.

III. Invisible Dual Loaded Scatterer

A similar modeling approach was used to simulate the scattering properties of an IDLS [25]. Unlike an ISLS (which cannot be modulated), an IDLS maintains the capability for modulation. As mentioned above, the geometry (load placement, etc.) of the scatterer design directly affects the induced current and subsequent scattered field. As such, two IDLS designs were considered: one following the traditional DLS design [6]-[7] where both loads (the PIN diode and inductor) are separated equidistantly from the center, illustrated in Fig. 5a and, referred to as the "equidistant IDLS" design, and a second (new) design where both loads are collocated at the center in a parallel configuration, illustrated in Fig. 5b and, referred to as the "collocated IDLS" design. The collocated IDLS design provides a load switching capability similar to what was done in [27] but with a different scatterer and loading circuit.

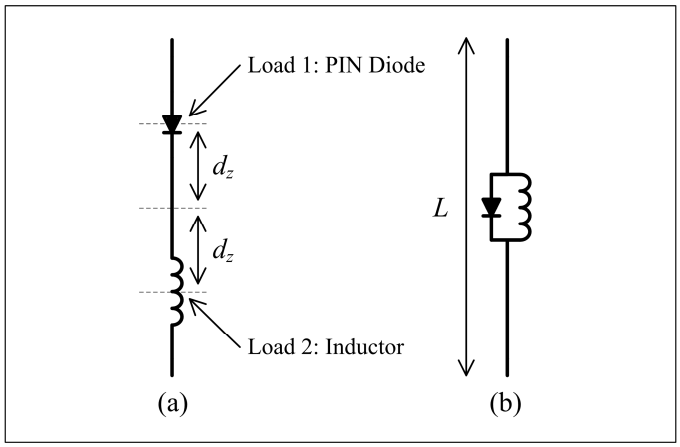

Fig. 5. Schematic of IDLS designs: (a) equidistant IDLS design, (b) collocated IDLS design.

A. Equidistant IDLS Design

The equidistant IDLS design was originally introduced in [22] and is based on previous work done in [6] and [7] with one of the PIN diodes (see Fig. 1b) replaced by an inductor, as shown in Fig. 5a. In order to determine the optimal (inductive) impedance necessary for electrical invisibility, simulations were conducted to study the effect of the inductor on the scattering properties of this design. The two loads were placed (equidistantly) a distance, d_z, of 15 mm (λ/8) from the center. The PIN diode was modeled (based on a Microsemi GC4270 PIN diode) as a resistance in series with an inductance (1.5 Ω and 0.6 nH respectively) during forward bias (FWD) and an inductance in series with a capacitance (0.6 nH and 0.2 pF respectively) during reverse bias (REV) [29]-[30]. This model for the PIN diode FWD and REV states was utilized for all relevant simulations presented herein. From the simulations, it was determined that a 36.6 nH inductor produced the optimal current distribution on the IDLS required to achieve electrical invisibility. This current distribution is shown in Fig. 6. For comparison, the current distribution along the length of a traditional MST scatterer (shown in Fig. 1a), referred to herein as a "traditional SLS", was simulated at the design frequency and is shown in Fig. 7.

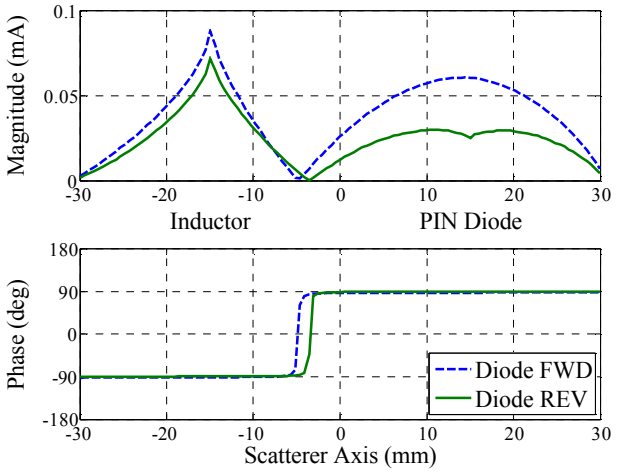

Fig. 6. Current induced along the equidistant IDLS (loads placed equidistant from the center).

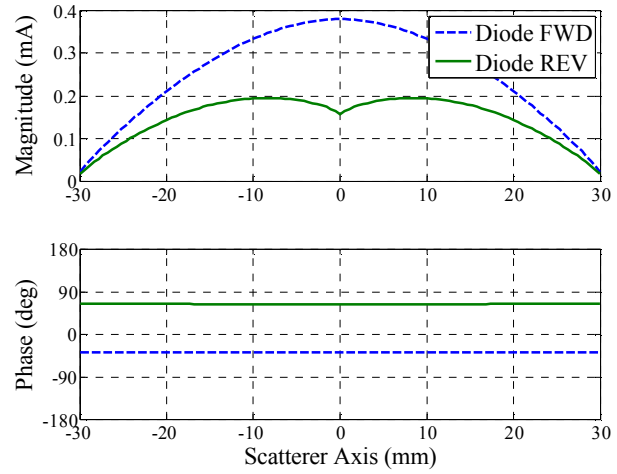

Fig. 7. Current induced along a traditional SLS.

From Fig. 6, it can be seen that the inductor causes a phase shift in the induced current, similar to the ISLS current of Fig. 3, only the inductor (and therefore the phase shift) has been offset -λ/8 (-15 mm) from the center of the scatterer (corresponding to the location of the inductive load). Likewise, at +λ/8 (15 mm), the effect of the diode can be clearly seen (similar to that shown in Fig. 7) as the current is

higher during the FWD state of the diode than during the REV state due to the low and high impedance of the respective diode states. As previously discussed, the phase shift caused by the inductor minimizes the integral of the induced current. In this case, it is evident from Fig. 6 that this phase shift is present for both states of the diode, indicating scattering from both states will be affected. The magnitudes of the scattered field for both diode states of the equidistant IDLS as a function of frequency are shown in Fig. 8.

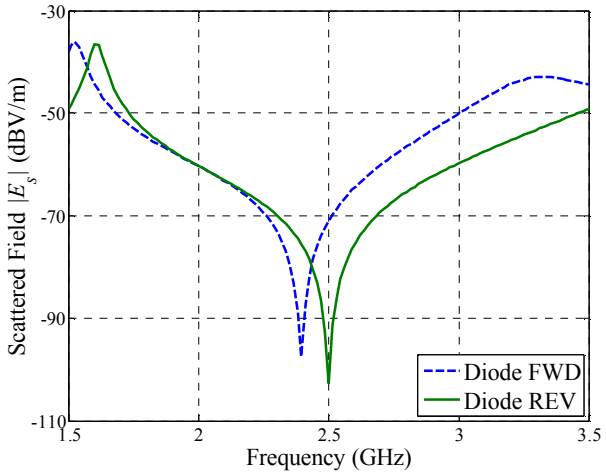

Fig. 8. Scattering from the equidistant IDLS design.

Since the objective of the equidistant IDLS design is to improve the MD of MST elements, (1) was used to calculate the MD using the simulated scattered fields (shown in Fig. 8) from this design. At the design frequency, an MD of 95% was calculated. For comparison, $|E_s|$ as a function of frequency for a traditional SLS was simulated and is shown in Fig. 9.

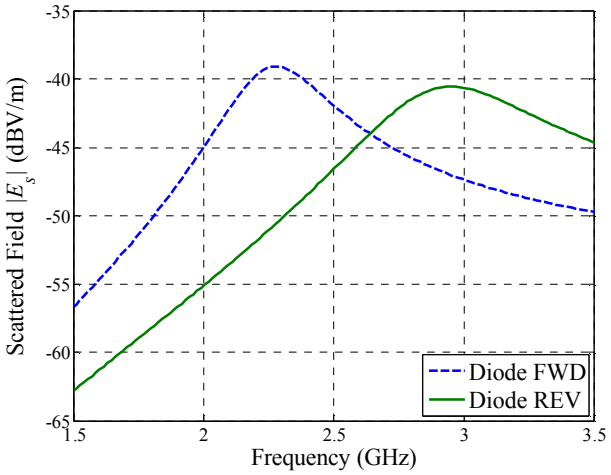

Fig. 9. Scattering from a traditional SLS.

Using the simulated results shown in Fig. 9, the modulation depth at 2.5 GHz was calculated using (1) to be 26%. However, as can be seen in Fig. 9, the MD could be improved by adjusting physical parameters of the scatterer so that the maximum scattering occurs at the design frequency (similar to [11]). In other words, the maximum difference between FWD and REV states occurs at 2.26 GHz. Using the results at this frequency, the MD for the traditional SLS is approximately 59%, which is better than the 26% MD at the design frequency but still less than the 95% MD achieved by the IDLS. Thus, the IDLS introduces a substantial improvement in modulation depth, which is quite significant as it relates to the detection of scattered signals for MST.

However, this improvement to the MD is not without practical drawbacks. When comparing the simulated results of the equidistant IDLS design (Fig. 8) to those of the traditional SLS (Fig. 9), it is evident that the phase shift in the induced current (caused by the inductive load) decreases the scattering during the REV state of the diode, which is desired. However, the phase shift also reduces $|E_s|$ during the FWD state of the diode, by more than 30 dB, when compared to the same state of the traditional SLS. This reduction in the FWD state scattering not only makes detection more difficult but could result in both scattering states effectively being invisible for less sensitive systems.

In addition, the inductor causes both states of the IDLS to have scattering nulls very close in frequency (see Fig. 8) which may also cause detection challenges (e.g. reliably distinguishing between the two states) for practical detection systems. Ultimately, these challenges may outweigh the improvements gained by increasing the MD. To this end, the second IDLS design, the collocated IDLS design, is discussed next.

B. Collocated IDLS Design

In an effort to mitigate the potential drawbacks of the equidistant IDLS design discussed above, the collocated IDLS design was created (shown in Fig. 5b). The intention of this design is that during the FWD (low impedance) state of the diode, the parallel combination of the collocated loads will resemble that of the SLS (Fig. 1a) in the same state, effectively removing the inductor and the subsequent phase shift in the induced current. Similarly, during the REV (high impedance) state of the diode, the reactive impedance of the inductor will dominate and the scatterer will resemble an ISLS, becoming electrically invisible (see Fig. 3). This design approach is similar to that of reconfigurable antennas [28].

As above, using the MM simulations, the optimal value for the reactive impedance (i.e., inductive load) to achieve electrical invisibility was determined. It was found that an inductance of 14 nH was optimum; which, when combined in parallel with the impedance of the REV state of the PIN diode resulted in a reactive impedance of approximately 764 Ω at the design frequency. This is the same impedance value required for electrical invisibility of an ISLS (discussed above), which is to be expected since the collocated IDLS design also loads the scatterer in the center (e.g., SLS) for electrical invisibility. In order to illustrate the effect of the collocated IDLS design, the current distribution at the design frequency (for both PIN diode states) is shown in Fig. 10.

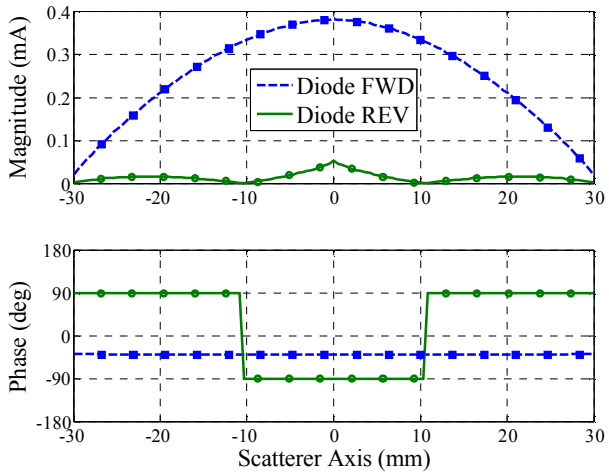

Fig. 10. Current induced along IDLS with loads collocated at the center.

It is evident from Fig. 10 that during the REV (high impedance) state of the diode, the current distribution of the collocated IDLS design matches that of an ISLS (SLS loaded with inductor only), which is shown in Fig. 3 and represented in Fig. 10 by circle markers. This current distribution was expected since the parallel combination of the REV diode and the 14 nH inductor resulted in the same reactive impedance (~764 Ω) of the ISLS in section II. Similarly, during the FWD (low impedance) state of the diode, the current distribution of the collocated IDLS design matches that of a traditional SLS during the same state of the diode, which is shown in Fig. 7 and represented in Fig. 10 by square markers. This correlation of the current distribution is attributed to the fact that the load impedance of the collocated IDLS, during the FWD diode state, matches that of the FWD diode only. From the results of the current distribution simulations (Fig. 10), it is expected that the scattering of the collocated IDLS will resemble that of a traditional SLS during the FWD state of the diode and that of an ISLS during the REV state of the diode. The magnitude of the simulated scattering, $|E_s|$, for this design is presented in Fig. 11 as a function of frequency.

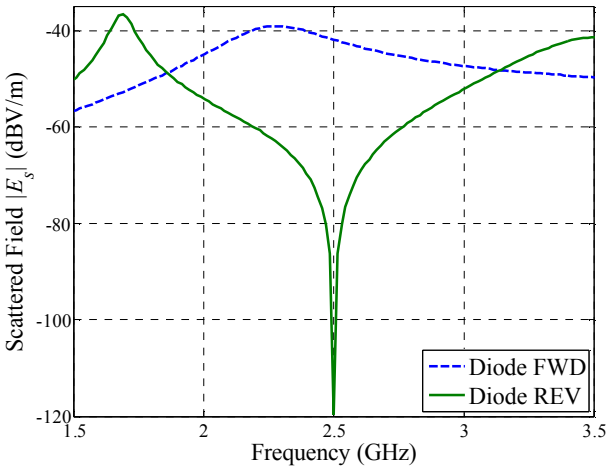

Fig. 11. Scattering from the collocated IDLS design.

As can be seen from Fig. 11 (and comparing to Fig. 9), the forward biased state of the PIN diode produces $|Es|$ identical to that of the traditional SLS for the same diode state. Further, the reverse biased state is minimized (invisible) at 2.5 GHz. This is expected from the current distribution shown in Fig. 10. Thus, the collocated IDLS provides the response of both a traditional SLS and ISLS, during the FWD and REV states of the diode respectively. Using the simulated results shown in Fig. 11 and (1), the MD at 2.5 GHz was calculated to be 99.9% (meaning the design effectively achieved electrical invisibility). Not only is the simulated MD for the collocated IDLS design improved as compared to the equidistant IDLS design (95% MD), but the possible measurement issues associated with the equidistant IDLS design have also been mitigated. More specifically, $|Es|$, during the FWD state of diode, no longer contains a scattering null and has substantially increased compared to the equidistant IDLS (by nearly 30 dB); therefore, less sensitive (i.e., lower cost) measurement equipment may be utilized **Error! Reference source not found.**.

IV. Measurements

In order to further investigate the application of electrically invisible antennas to MST, a collocated IDLS was constructed and measured at 2.5 GHz. A traditional SLS was also constructed and measured for comparison purposes.

A. Scatterer Fabrication

The IDLS was fabricated from 24 AWG wire sections cut such that once soldered to the load the length was approximately λ/2 (60 mm at 2.5 GHz). The scatterer was centrally loaded with a Microsemi GC4270 PIN diode in parallel with a 15 nH surface mount inductor (0201 package size). This inductance is slightly higher than the optimal value (14 nH) and hence some slight variation is expected in the frequency at which electrical invisibility is achieved. For this reason, swept frequency measurements were conducted from 1.5 to 3.5 GHz, in order to ensure the invisible state of the IDLS response was measured.

Small biasing wires (36 AWG) were connected at the ends of the scatterer to deliver the DC biasing current necessary for PIN diode modulation. These biasing wires were connected through ferrite chips in order to block any high frequency currents resulting from the scatterer. Additionally, a 0.22 μF capacitor (0201 package size) was included in series with the inductor to block the PIN diode DC biasing currents from saturating the inductor. A relatively high capacitance was chosen so that the impedance of the capacitor would be negligible at the measurement frequencies (i.e., GHz range).

A design frequency of 2.5 GHz was selected based on component availability. Specifically, appropriate inductors with a self-resonance frequency (SRF) above 2.5 GHz are commercially available. This is important to consider when selecting load inductors since when operating near and above the SRF, the impedance of the inductor varies greatly from the intended value. The typical SRF (specified by the manufacturer) for the 15 nH inductor used for the IDLS is 6.6

GHz [31], which results in an impedance variation of approximately 50Ω from ideal at the design frequency. This variation will also contribute to the deviation of the IDLS scattering null from the design frequency.

For purposes of comparison, a traditional SLS was also constructed. This SLS utilized the same wire, PIN diode, and biasing circuitry as the contrasted IDLS.

B. Measurement Setup

To conduct measurements, each scatterer was placed (individually) on a structure of very low permittivity foam (i.e., resembling free-space), approximately 0.5 m from the aperture of two 1-4 GHz ridged horn antennas inside a measurement enclosure (semi-anechoic chamber), as illustrated in Fig. 12.

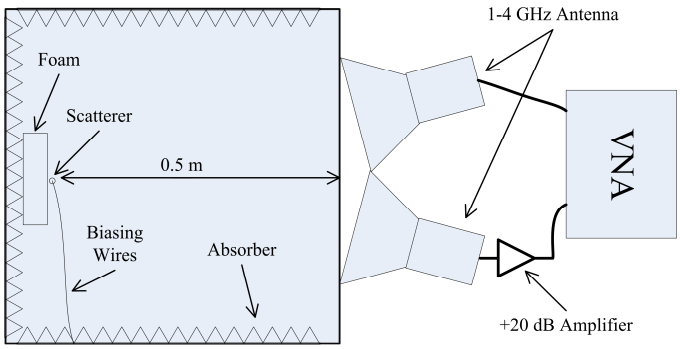

Fig. 12. Schematic of measurement setup used when measuring the scattered fields of the MST scatterers.

The horn antennas were each connected to a calibrated port of an Agilent 8753E Vector Network Analyzer (VNA). A bistatic setup was chosen for better measurement sensitivity, since the scattering from the DUT is relatively weak. More specifically, a bistatic setup allows for the inclusion of a low noise pre-amplifier (+20 dB gain) at the receiving port (shown in Figure 4.8), which increases the signal to noise ratio (SNR) of the measurement. Additionally, the transmission uncertainty (i.e., S21 error) of the VNA is much lower than the reflection uncertainty (i.e., S11 error) when measuring small signals [33]. Swept-frequency measurements of the complex transmission coefficient, S21 (related to $|E_s|$), were made, along with an ambient measurement (i.e., measurement setup without the presence of a scatterer). In this way, the scattered field from the scatterer may be determined by coherently subtracting the ambient measurement from that with the scatterer present. This technique does not, however, remove the scattering from the PIN diode biasing wires (shown in Fig. 12). Due to the biasing wires' small size (36 AWG) and normal orientation to the polarization of the incident electric field, the amount of scattering is assumed to be minimal, but may still interfere with the deep null (i.e. invisible state) of the IDLS response. In order to investigate this issue, high frequency absorber material was used to cover approximately half of the biasing wire inside the measurement enclosure during one set of measurements.

C. Results

After coherent background subtraction of the measured S21 data, the resulting response of the collocated IDLS and the traditional SLS are presented in Fig. 13 and Fig. 14 respectively.

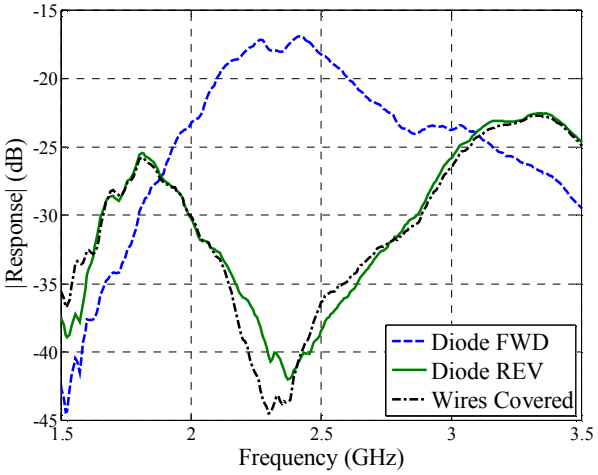

Fig. 13. Measured response of collocated IDLS.

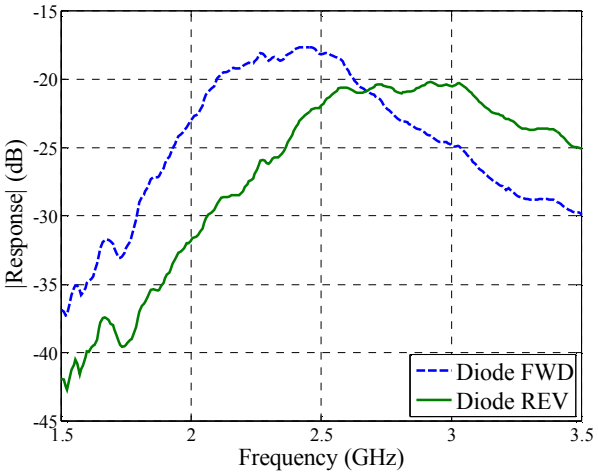

Fig. 14. Measured response of traditional SLS.

Upon comparison of the results presented in Fig. 13 and Fig. 14, it is immediately evident that the IDLS (Fig. 13) results in a significant improvement to the MD as compared to the traditional SLS (Fig. 14). At the design frequency of 2.5 GHz, the IDLS achieves an MD of 82%, whereas an MD of 21% is achieved using the traditional SLS. As expected, the scattering null (i.e., invisible state) was slightly shifted from the design frequency, which is most likely attributed to the variations in the inductor values discussed above. That is to say, the maximum MD for the IDLS of 88% occurred at 2.37 GHz. Although 88% MD is significant, it is still less than the simulated value for the collocated IDLS in section III.B (99.9%). This difference is attributed in part to the scattering by the small wires used to bias the PIN diode (which is not removed by the coherent background subtraction). By reducing the scattering from the diode biasing wires (e.g., covering the wires with absorbing material), a slightly better

MD of 91% (at 2.3 GHz) is achieved (see Fig. 13). Due to the fact that the scattering by the PIN diode biasing wires is a static reflection (i.e., not affected by the PIN diode modulation state), it may be possible to mitigated its effects by further processing (e.g., time domain analysis), or different (advanced) measurement techniques.

Overall, it is evident that the new IDLS design significantly improved the MD as compared to a traditional MST element. However, the measurements proved to be quite sensitive to variation in component values indicating that precise fabrication methods and components are required to achieve maximum MD (i.e., a scattering null) at the frequency of interest.

V. Concluding Remarks

In this paper, a new MST scatterer design (collocated IDLS) which has the ability to modulate between both visible (scattering) and invisible (minimal scattering) states was proposed, simulated, and successfully measured. Simulations showed this new design to be (theoretically) capable of achieving 99.9% modulation depth. Measurements showed a maximum modulation depth of 91%. This discrepancy is partially attributed to the measurement technique which included the effects of the load (PIN diode) biasing wires. Performance may be improved with more precise measurement techniques and/or more precisely fabricated scatterers. However, achieving the maximum theoretical result is unlikely due to losses in practical implementations (e.g., finite conductivity of the scatterers, etc.) which were not taken into account by the simulations. Even so, the new design was shown to significantly improve modulation depth (82%) when compared to that achieved by a traditional MST scatterer (26%) at the design frequency (2.5 GHz). Further investigation found that the new design achieved a MD of 91% slightly off from the design frequency at 2.3 GHz. This discrepancy is attributed to differences between the simulation and the constructed scatterer (i.e., a practical inductor was used in the scatterer fabrication as opposed to an ideal inductor used in the simulation).

Future work may include the fabrication of such scatterers using PCB technology in order to achieve maximum MD at the design frequency. Removing the dependency on lumped elements may also be possible with PCB-based scatterers (e.g., printed spirals [14]). Additionally, as discussed above, this new scatterer design technique may find application in MST array configurations, RFID tag designs, and materials characterization.

References

[1] Bolomey, J.C. and F.E. Gardiol, Engineering Applications of the Modulated Scatterer Technique, Artech House, Norwood, MA, 2001.

[2] Abou-Khousa, M.A., "Novel Modulated Antennas and Probes for Millimeter Wave Imaging Applications," Ph.D. Dissertation, Electrical and Computer Engineering Department, Missouri University of Science and Technology, Rolla, MO 65409, April 2009.

[3] Hughes, D. and R. Zoughi, "A Novel Method for Determination of Dielectric Properties of Materials Using a Combined Embedded Modulated Scattering and Near-field Microwave Techniques - Part II. Dielectric Property Recalculation", *IEEE Transactions on Instrumentation and Measurement*, vol. 54, no. 6, pp. 2398-2401, December 2005.

[4] Freiburger, G.S. and R. Zoughi, "Dielectric Material Characterization by Complex Ratio of Embedded Modulated Scatterer Technique States," Proceedings of the IEEE Instrumentation and Measurement Technology Conference, pp. 67-71, Ottawa, Canada, May 16-19, 2005.

[5] Harrington, Roger F., "Small Resonant Scatterers and Their Use for Field Measurements," *Microwave Theory and Techniques, IRE Transactions on* , vol.10, no.3, pp.165,174, May 1962

[6] Abou-Khousa, M. A., K. M. Donnell and R. Zoughi, "Robust Embedded Probe Utilizing Dual-Loaded Modulated Linear Scatterers," Proceedings of the 4th International Conference on Electromagnetic Near-Field Characterization & Imaging, pp. 28-32, Taipei, Taiwan, 24 – 26 June 2009.

[7] Donnell, K. M., M. A. Abou-Khousa, M. Belayneh, and R. Zoughi, "Dual-Loaded Modulated Dipole Scatterer as an Embedded Sensor," *IEEE Transactions on Instrumentation and Measurement*, vol. 60, no. 5, pp. 1884-1892, 2011.

[8] Donnell, K.M.; Zoughi, R., "Application of Embedded Dual-Loaded Modulated Scatterer Technique (MST) to Multilayer Structures," *IEEE Transactions on Instrumentation and Measurement*, vol.61, no.10, pp.2799,2806, Oct. 2012

[9] A.D. Skinner, "Modulation: fundamental techniques for traceability," IEE Colloquium on Accreditation of RF Measurement, pp. 6/1 - 6/6, Feb. 1993.

[10] Bolomey, J.C., et al., "Rapid near-field antenna testing via arrays of modulated scattering robes," *IEEE Transactions on Antennas and Propagation*, vol. 36, no. 6, pp. 804-814, June 1988.

[11] Bolomey, J.-C.; Memarzadeh-Tehran, H.; Laurin, J.-J., "Optimization of Optically and Electrically Modulated Scattering Probes for Field Measurements," *IEEE Transactions on Instrumentation and Measurement*, vol.63, no.1, pp.154,165, Jan. 2014

[12] J.Ch. Bolomey et al., "Electromagnetic Modeling of RFID-Modulated Scattering Mechanism. Application to Tag Performance Evaluation", Proceedings of the IEEE, vol. 98, no. 9, pp. 1555-1569, Sept. 2010.

[13] P.V. Nikitin, K.V.S. Rao, and R.D. Martinez, "Differential RCS of RFID Tag", Electronics Letters, vol. 43, no. 8, pp. 431-432, April 2007.

[14] H. Memarzadeh-Tehran, J.-J. Laurin, and R. Kashyap, "Optically modulated probe for precision near-field measurements," IEEE Trans. Instrum. Meas., vol. 59, no. 10, pp. 2755–2762, Oct. 2010.

[15] Iigusa, K., T. Sawaya, M. Taromaru, T. Ohira, and B. Komiyama, "Experimental Proof of Electrically Invisible State of Inductively Loaded Dipole and Proposal of Electrically Invisible Meander-Lines", *IEEE Transactions on Antennas and Propagation*, vol. 54, no. 11, pp. 3374-3382, November 2006.

[16] Iigusa, K., T. Ohira, and B. Komiyama, "An Electrically Invisible Dipole Loaded with a Variable Reactor and Its Applications for a Reconfigurable Antenna", Electronics and Communications in Japan – Part 1, vol. 89, no. 3, pp. 21 – 35, 2006.

[17] Chen, K.M., and V. Leipa, "The Minimization of the Back Scattering of a Cylinder by Central Loading", *IEEE Transactions on Antennas and Propagation*, pp. 576 – 582, 1964.

[18] Iigusa, K., T. Ohira, and B. Komiyama, "An Equivalent Weight Vector Model of Array Antennas Considering Current Distribution along Dipole Elements", Electronics and Communications in Japan – Part 1, vol. 89, no. 2, pp. 22 – 35, 2006.

[19] Iigusa, K.I., T. Ohira, and B. Komiyama, "Electrically-invisible Parasitic Dipoles for New Reconfigurable Array Antennas," in Proc. APMC2004, Dec. 2004, p. 694.

[20] Glaser, J.I., "Stealthy Antennas: Minimizing the Radar Cross Section of an Essential Communication System Component", The WSTIAC Quarterly, vol. 8, no. 2,pp. 11-14.

[21] Iigusa, K., H. Harada, S. Kato, J. Hirokawa, and M. Ando, "Radio-Wave Transparent Surface Containing Lines Loaded with Impedance at Regular Intervals", IEEE Antennas and Propagation Society International Symposium, pp. 3960-3963, 2007.

[22] Crocker, D.A.; Donnell, K.M., "Application of electrically invisible antennas to the Modulated Scatterer Technique," Instrumentation and Measurement Technology Conference (I2MTC), 2013 IEEE International , vol., no., pp.392,396, 6-9 May 2013

[23] C. A. Balanis, Antenna Theory and Techniques: Analysis and Design, 2nd ed. New York: Wiley, 1997.

[24] Orfanidis, Sophocles J. Electromagnetic Waves and Antennas, Piscataway: ECE Department Rutgers University, 2010. Rutgers University, March 2013, <http://www.ece.rutgers.edu/~orfanidi/ewa/>.

[25] Harrington, R. F, Field Computations by Moment Methods, IEEE Press Series on Electromagnetic Waves, Donald G. Dudley, Series Editor, 1993.
[26] A. J. Poggio, and R. W. Adams, “Approximations for Terms Related to the Kernel in Thin-wire Integral Equations,” UCRL-51985, Lawrence Livermore Lab., Livermore, CA, Dec. 1975.
[27] Capdevila, S.; Jofre, L.; Romeu, J.; Bolomey, J.C., "Multi-Loaded Modulated Scatterer Technique for Sensing Applications," *IEEE Transactions on Instrumentation and Measurement*, vol.62, no.4, pp.794,805, April 2013
[28] Fallahpour, M.; Ghasr, M.T.; Zoughi, R., "A multiband reconfigurable CPW-fed slot antenna," Antennas and Propagation Society International Symposium (APSURSI), 2012 IEEE , vol., no., pp.1,2, 8-14 July 2012
[29] Microsemi, MicroSolutions – Microwave Diode Packages, Know What You Are Getting, K. R. Philpot, Microsemi-Lowell.
[30] Microsemi, MicroNote Series 701, PIN Diode Fundamentals, B. Doherty, Microsemi-Watertown.
[31] Abou-Khousa, M.A.; Baumgartner, M.A.; Kharkovsky, S.; Zoughi, R., "Novel and Simple High-Frequency Single-Port Vector Network Analyzer," *IEEE Transactions on Instrumentation and Measurement*, vol.59, no.3, pp.534,542, March 2010
[32] TDK Corporation, [Online], Available: http://www.tdk.co.jp/tefe02/e521_mlk.pdf Accessed: Jan. 2014
[33] Agilent Technologies, Inc, [Online], Mar. 2014, Available: <http://cp.literature.agilent.com/litweb/pdf/5968-5160E.pdf>